Soil moisture controls on canopy-scale water and carbon fluxes in an African savanna

Christopher A. Williams[1]

Nicholas School of the Environment and Earth Sciences, Duke University, Durham, North Carolina, USA

John D. Albertson

Department of Civil and Environmental Engineering, Duke University, Durham, North Carolina, USA

[1] Tower-based measurements of mass and energy exchanges at the end of the growing season in central Botswana were used to evaluate functional relationships commonly applied to predict water and carbon fluxes between savanna landscapes and the atmosphere. Following a large rainfall event, daily evapotranspiration (ET_{daily}) exhibited an exponential decay consistent with a derived analytical expression based on critical and wilting-point soil moisture limits for savanna vegetation native to the study region. A piecewise linear soil moisture limitation function provided good estimates of ET_{daily} as a function of potential evapotranspiration and soil moisture ($R^2 = 0.92$). Comparison of a soil moisture mass balance with measured ET_{daily} indicated deeper root water uptake at a site with more woody vegetation compared with a grass-dominated site. Linear correlation ($R^2 = 0.90$) of daytime CO_2 flux and evapotranspiration supported a constant water use efficiency to estimate carbon fluxes from water fluxes. Daytime and nighttime CO_2 fluxes responded similarly to soil drying, enabling estimation of total daily CO_2 flux from ET_{daily}. These experimental results support a simple model of savanna land-atmosphere exchange over interstorm periods.   *INDEX TERMS:* 1818 Hydrology: Evapotranspiration; 3322 Meteorology and Atmospheric Dynamics: Land/atmosphere interactions; 1866 Hydrology: Soil moisture; 1878 Hydrology: Water/energy interactions; *KEYWORDS:* African savanna, evapotranspiration, land-atmosphere exchange, soil moisture, water and carbon flux, water limitation

Citation: Williams, C. A., and J. D. Albertson (2004), Soil moisture controls on canopy-scale water and carbon fluxes in an African savanna, *Water Resour. Res.*, *40*, W09302, doi:10.1029/2004WR003208.

1. Introduction

[2] Savannas cover a large fraction of the terrestrial landscape, including as much as 50% of the African continent and 20% of the global land cover [*Atjay et al.*, 1979]. Recent debate highlights their uncertain role in global carbon and water cycles [*Fisher et al.*, 1994; *Jeltsch et al.*, 2000; *Cao et al.*, 2001; *Jackson et al.*, 2002]. Savannas are defined broadly by the coexistence of woody (or tree) and herbaceous (or grass) vegetation and classified more specifically by their relative amounts of each of these plant functional types (PFTs). The functional relationships between environmental state variables and vegetation-atmosphere water and carbon exchange rates are notably different for the two PFTs [*Scholes and Walker*, 1993; *Smith et al.*, 1997]. Consequently, attempts to model the aggregate landscape surface fluxes must account for the relative amounts of each PFT present and their contrasting functional dependence on environmental state variables, such as soil moisture.

[3] Soil moisture is well established as a dominant control on savanna productivity and, consequently, as a primary driver of composition, structure, and distribution of vegetation cover [*Scholes and Parsons*, 1997; *Rodriguez-Iturbe et al.*, 1999a, 1999b; *Smit and Rethman*, 2000], as evidenced by strong, positive correlation between large-scale spatial patterns in mean annual precipitation and savanna productivity, or vegetation cover [*Le Houerou and Hoste*, 1977; *Rutherford*, 1980]. Water loss by vegetation is strongly coupled with carbon gain in savannas, as shown from observations conducted at the canopy scale [*Le Roux and Mordelet*, 1995; *Verhoef et al.*, 1996; *Moncrieff et al.*, 1997; *Eamus et al.*, 2001; *Scanlon and Albertson*, 2003a] and leaf scale [*Ferrar*, 1980; *Scholes and Walker*, 1993; *Eamus and Cole*, 1997; *Prior et al.*, 1997]. These general features of savanna water and carbon exchanges have been incorporated into modeling efforts. However, many models currently employed to predict savanna water use or productivity rely on assumptions that could benefit from additional examination with empirical results investigating their applications at the specific space and time scales of the models. For example, *Rodriguez-Iturbe et al.* [1999a, 1999b, 2001] adopt a piecewise linear soil moisture limitation function on evapotranspiration as a central assumption employed in modeling probabilistic soil moisture dynamics. They support this simplification by citing studies that document soil moisture limitation of leaf conductance or stand transpiration for a range of plant

---

[1] Also at Department of Civil and Environmental Engineering, Duke University, Durham, North Carolina, USA.

functional types including temperate forests, a sclerophyllous woody shrub, a temperate zone cereal grain, a Douglas fir stand, and plants of the Patagonian steppe [*Federer*, 1979; *Spittlehouse and Black*, 1981; *Gollan et al.*, 1985; *Schulze*, 1993; *Paruelo and Sala*, 1995]. The works cited by *Rodriguez-Iturbe et al.* [1999a, 1999b, 2001] and *Laio et al.* [2001] do not specifically document soil moisture limitation of evapotranspiration for savannas, and may benefit from explicit examination with observational data at the daily, canopy scale, as presented in this study.

[4] Models that operate at the daily and canopy scales [e.g., *Jolly and Running*, 2004; *Rodriguez-Iturbe et al.*, 1999a, 1999b, 2001] typically rely on instantaneous, leaf-scale observations for characterizing functional dependencies of daily, canopy-scale processes. This assumes that leaf-scale functional responses to environmental conditions are representative of canopy-scale responses. Despite the known complexity typical of scaling biological exchanges [*Norman*, 1993], the structure and function of some ecosystems may enable reasonable estimation of canopy water and carbon exchanges from scaling leaf-scale observations linearly with vegetation density, such as grasslands, which typically have well-mixed canopy atmospheric conditions that are tightly coupled to conditions above the canopy [*McNaughton and Jarvis*, 1983, 1991; *Larcher*, 1995]. An additional common simplification used in modeling carbon exchanges in savanna is to assume a constant, linear relationship between carbon gain and transpiration over daily to annual timescales [*Walker et al.*, 1981; *van Langevelde et al.*, 2003], despite observed diurnal, daily, and seasonal trends in water use efficiency (*WUE*) [*Jones*, 1983; *Verhoef et al.*, 1996; *Moncrieff et al.*, 1997; *Scanlon and Albertson*, 2003a].

[5] We report results from a month-long field campaign conducted in the Kalahari Desert near Ghanzi, Botswana. Vegetation of this semiarid savanna is acutely sensitive to water limitation and responds rapidly to changes in water availability, providing an appropriate setting for resolving soil water controls on plant-atmosphere exchanges [*Scholes and Parsons*, 1997]. In addition, coarse, sandy soils underlying the Ghanzi site [*Baillieul*, 1975] allow us to adopt assumptions regarding infiltration and drainage that simplify the interpretation of measured fluxes and states [*Scanlon and Albertson*, 2003b].

[6] In this paper we examine the temporal course of canopy-scale evapotranspiration (*ET*, kg H_2O m^{-2} s^{-1}) and CO_2 exchange (*Fc*, mg CO_2 m^{-2} s^{-1}) associated with soil moisture drydown following a large rain event for two adjacent sites: one dominated by grasses and another containing a tree fractional cover representative of savanna in the region. We focus our analysis on key fluxes and states that characterize changes in vegetation water and carbon exchanges in response to drydown. More specifically, we investigate soil moisture limitation of *ET*, the resulting shape of the decay of *ET* with time since rainfall, whether scaling leaf exchanges based on linear weighting of vegetation density agrees with canopy-scale exchanges, and the temporal dynamics of *WUE*. These results are examined in the context of typical model formulations for savanna water and carbon exchange [*Rodriguez-Iturbe et al.*, 1999a,

Table 1. Soil Hydraulic Properties for the Ghanzi Savanna, Where Ks Is Saturated Hydraulic Conductivity, θs Is the Saturated Volumetric Soil Water Content, ψ_e Is the Air Entry Matric Potential, and b Is an Empirical Parameter in the *Clapp and Hornberger* [1978] Model

Parameter	Unit	Value
Ks	mm/d	2000
θs	m^3/m^3	0.4
ψ_e	mm	−121
b	...	4.05

1999b; *Verhoef and Allen*, 2000; *Rodriguez-Iturbe et al.*, 2001].

2. Theoretical Background

[7] We briefly introduce three theories regarding soil moisture controls on water and carbon fluxes in savannas. Subsequently, each theory is addressed with observations taken from the Ghanzi field site during the month-long experiment.

2.1. Soil Moisture Control on *ET*

[8] Evapotranspiration (*ET*) is commonly estimated as a moisture-limited fraction, $\beta(\theta)$ [*Jacquemin and Noilhan*, 1990; *Avissar and Pielke*, 1991; *Mahfouf et al.*, 1996; *Rodriguez-Iturbe et al.*, 1999b; *Albertson and Kiely*, 2001], of a potential rate, *PET* [kg m^{-2} s^{-1}], as

$$ET = PET\beta(\theta)f_v, \tag{1}$$

where f_v is the fractional cover of vegetation. Because of the low surface soil moisture states, we are implicitly assuming that the bare soil fraction $(1 - f_v)$ does not contribute significantly to *ET*. We adopt the piecewise linear moisture limitation function

$$\beta(\theta) = \begin{cases} 1 & \text{for } \theta \geq \theta_{cr} \\ \dfrac{\theta - \theta_{wilt}}{\theta_{cr} - \theta_{wilt}} & \text{for } \theta_{wilt} < \theta < \theta_{cr}, \\ 0 & \text{for } \theta \leq \theta_{wilt} \end{cases} \tag{2}$$

where θ is volumetric soil moisture and critical (θ_{cr}), and wilting-point (θ_{wilt}) soil moisture limits can be obtained by transforming critical and wilting-point water potentials for savanna tree and grass PFTs [*Scholes and Walker*, 1993; *Mahfouf et al.*, 1996; *Rodriguez-Iturbe et al.*, 1999a, 1999b] to corresponding soil moisture limits. The *Clapp and Hornberger* [1978] relationships are used to relate matric potential to soil moisture with the parameters listed in Table 1 (obtained from *Campbell and Norman* [1998]). *PET* is estimated with the *Priestley and Taylor* [1972] formulation

$$PET = \left[\alpha(Rn - G)\frac{\Delta}{\Delta + \gamma}\right]\frac{1}{Lv}, \tag{3}$$

where $\alpha(=1.26)$ accounts for large-scale advection and entrainment, Rn [W m^{-2}] is net all-wave radiation, G [W m^{-2}] is soil heat flux, $\gamma(=0.67$ mbar $°C^{-1})$ is the psychrometric constant, $Lv(=2.45 \times 10^6$ J $kg^{-1})$ is the latent

heat of vaporization, and Δ [mbar $°C^{-1}$] is the slope of the saturation vapor pressure curve [*Campbell and Norman*, 1998]. In section 4.6 we evaluate equations (1)–(3) in the context of our soil moisture and flux data.

2.2. Evapotranspiration Decay in Time

[9] An alternative to modeling *ET* with equation (1) is to estimate *ET* as a function of time since a wetting event by analogy to a desorption-limited process [*Shouse et al.*, 1982; *Brutsaert and Chen*, 1995, 1996]. A simple two-stage model has been shown to provide a good characterization of evaporation from a bare soil following a wetting event, where the first stage describes the period over which evaporation equals the potential rate and the second stage is initiated when the evaporation becomes fully controlled by resistances that limit the rate of soil water movement to the surface [*Brutsaert*, 1982; *Parlange et al.*, 1992]. The second stage is characterized by a power law decay of evaporation (*E*, mm d^{-1}) with time [*Gardner*, 1959; *Brutsaert*, 1982; *Parlange et al.*, 1985; *Parlange et al.*, 1992], obtained from a similarity solution of Richard's equation for desorption [*Bruce and Klute*, 1956], yielding

$$E = \frac{1}{2} De (t - t_*)^{1/2}, \qquad (4)$$

where *De* is the desorptivity constant related to the soil diffusivity and t_* is the time at which *E* departs from *PET* [*Gardner*, 1959; *Brutsaert*, 1982; *Parlange et al.*, 1985; *Parlange et al.*, 1992]. This simple two-stage model has also been applied to estimate evapotranspiration from vegetated surfaces, which is a nontrivial extension because transpiration is influenced by plant water extraction that adapts to water availability throughout a spatially distributed rooting volume, not just at the surface, and plants exert an added resistance from stomatal limitation [*Jones*, 1983; *Larcher*, 1995]. Despite this complication, the two-stage model was shown to provide reasonable estimates of the time rate of decay of *ET* from a cowpea field [*Shouse et al.*, 1982], and a natural tallgrass prairie during a thorough, natural drying [*Brutsaert and Chen*, 1995, 1996]. With its minimal parameterization, this model might potentially be useful for estimating plant transpiration in water-limited savannas. Such an interstorm model would be analytically tractable, allowing us to obtain *ET* estimates from a stochastic rainfall description and a deterministic decay of soil moisture, similar to the work of *Rodriguez-Iturbe* [1999a, 2001]. In section 4.7 we explore the skill of this two-stage model in estimating *ET* for the Ghanzi savanna and introduce an alternative, analytical model that we show to be both more consistent with equations (1) and (2) and with the data presented below.

2.3. Water Use Efficiency

[10] Mechanistic coupling of transpiration with photosynthesis suggests that we may obtain estimates of *Fc* from *ET* with an efficiency describing the amount of carbon gained for each unit of water lost [*Jones*, 1983; *Larcher*, 1995]. In this study we define canopy-scale *WUE* [kg CO_2 kg^{-1} H_2O] as

$$WUE = \frac{Fc}{ET} \eta, \qquad (5)$$

where $\eta = 10^{-6}$ in order to clear the units. By definition of the field-scale fluxes, equation (5) includes contributions from both soil and vegetation sources/sinks of CO_2 and H_2O. However, if canopy fluxes of water and carbon are much greater than soil fluxes, as we might expect in a region such as the Kalahari with low soil moisture and carbon content, then the soil fluxes can be ignored and *WUE* may be estimated from stomatal diffusion considerations. Furthermore, in section 4.8 we study the temporal trend of measured canopy-scale *WUE* through the drydown to investigate whether *WUE* can be approximated as a constant at the daily timescale over the interstorm period, as needed to extend an analytical model of interstorm *ET* into a model of interstorm *Fc*. We compare *Fc* estimates to those measured in section 4.9.

3. Methods

[11] The experiment was conducted on the Dqae Qare reserve, located approximately 24 km northeast of Ghanzi, Botswana, from 5 March to 8 April 2002, at the end of the wet (growing) season that typically lasts from December through March. Monthly precipitation records from 1922 to 1989 for Ghanzi report mean annual precipitation of 400 mm with 75 mm delivered typically in March [*National Climate Data Center*, 2003]. Two sites were selected less than 2 km apart for intensive measurements, one with an herbaceous canopy composed primarily of grass, the grass site (subscript *g*), and one with herbaceous vegetation mixed with a tree cover representative of the region, the mixed site (subscript *m*).

[12] We installed two instrument towers and equipped them to measure three components of velocity providing a mean horizontal wind speed (*u*, m s^{-1}), air temperature (T_a, °C), air CO_2 concentration, and specific humidity (q_a, g water vapor kg^{-1} moist air) at 10 Hz with a triaxial sonic anemometer (CSAT3, Campbell Scientific) and an open-path CO_2/H_2O infrared gas analyzer (7500, LI-COR) located 8 m above the ground at the mixed site and 2 m above the ground at the grass site. Half-hour averaged fluxes of momentum, sensible heat (*H*, W m^{-2}), latent heat (*LE*, W m^{-2}), and carbon dioxide (*Fc*) from eddy covariances were calculated as well as basic turbulence and micrometeorological statistics. All mass fluxes are reported with the standard micrometeorological convention of positive, indicating an upward flux from the land to the atmosphere. We used standard quality assurance and quality control for eddy covariance measurements including the accepted practices of tilt correction, filtering spikes, and applying the Webb correction [*Webb et al.*, 1980; *Kaimal and Finnigan*, 1994]. All references to time of day are local standard time. Incoming and outgoing shortwave and longwave radiation were measured with a radiometer (CNR1, Kipp and Zonen) mounted at the top of each tower. Soil heat flux (*G*, W m^{-2}) was measured with four heat flux plates at each site (HFT3, Campbell Scientific), and vertical profiles of volumetric soil moisture content were measured with reflectometer probes (CS615, Campbell Scientific) installed horizontally at depths of 5, 15, 30, and 50 cm within tree, grass, and bare soil plots at the mixed site, and only grass and bare soil plots at the grass site. Near-surface soil temperatures, measured with copper-constantan thermocouples, and soil moisture were used to

Table 2. Fractional Covers of Tree (f_t), Herbaceous (f_h), Bare Soil (f_b), and Total Vegetation (f_v) for the Grass and Mixed Sites in Open Patches, Beneath Tree Canopies (Closed), and as a Total Fraction of Areal Coverage, With Plus or Minus the Standard Deviation

Site	Canopy	f_t	f_h	f_b	f_v
Grass	open	...	0.76 ± 0.19	0.24 ± 0.12	0.76 ± 0.19
Grass	closed	...	0.78 ± 0.20	0.22 ± 0.13	1
Grass	areal	0.05	0.72	0.23	0.77
Mixed	open	...	0.63 ± 0.18	0.37 ± 0.16	0.63 ± 0.18
Mixed	closed	...	0.70 ± 0.26	0.30 ± 0.22	1
Mixed	areal	0.20	0.51	0.29	0.71

Table 3. Leaf Area Characteristics of the Grass and Mixed Sites, Including Mean and Maximum (in Parentheses) Values, With Plus or Minus the Standard Deviation

Characteristic	Value
LAI_{veg} grass	1.1 (2)
LAI_{veg} tree	2.0 (4)
LAI_{areal} grass site	1.1 ± 0.9
LAI_{areal} mixed site	0.7 ± 0.4

correct G for soil heat storage effects [*Cellier*, 1996]. Infrared temperature sensors (IRTS-P, Apogee Instruments) were used to measure leaf and soil skin temperatures. Energy balance closure, determined from the slope of the linear regression of $H + LE$ versus $Rn - G$, was 0.92 and 0.79 at the grass and mixed sites with intercepts of less than 15 W m^{-2} and $R^2 = 0.98$.

[13] In addition to canopy-scale observations, we measured, at certain times, the leaf-scale CO_2 assimilation (A, mg m^{-2} s^{-1}), transpiration, and leaf temperature with a portable CO_2/H_2O infrared gas analyzer (6200, LI-COR). Leaf-level observations were conducted during select daylight hours on leaves of *Acacia erioloba*, *Combretum* spp., *Terminalia sericea*, and *Eragrostis pallens* and *E. lehmaniana*. Intercepted photosynthetically active radiation was measured with a ceptometer (model SF-80, Decagon Devices) on a regularly spaced grid of points, with 40 observations at the mixed site and 90 observations at the grass site, located within 100 m of each tower in diffuse light conditions both above and under the vegetation canopy to obtain estimates of leaf area index spatially averaged at the canopy scale (LAI_{areal}, m^2 leaf area per m^2 ground area), and additional measurements within grass or tree patches to estimate the leaf area index of specific vegetation functional types (LAI_{veg} m^2 of leaf area per m^2 vegetated area), as described by *Norman and Campbell* [1989]. Visual assessments of bare soil, herbaceous, and tree fractional covers in each tower footprint were obtained from viewing 10 m × 10 m grids with 100 observations at the mixed site and 36 observations at the grass site. Tree canopy cover was measured using a spherical densiometer. The number of grass roots and broad-leaved tree roots were each counted in three trenches excavated near the base of *Terminalia* and *Acacia* trees. Roots were counted in three profiles for each trench and divided into vertical bands of 0.15 m (1 m wide) to a depth of 1.05 m below the surface following a procedure outlined by *Caldwell and Virginia* [1989].

4. Results and Discussion

4.1. Vegetation Structure

[14] The relative components of the different PFTs and bare soil covers at each of the two sites are listed in Table 2, and the leaf area characteristics of the sites are listed in Table 3. Sample standard deviations in vegetation fractional cover (Table 2) and LAI (Table 3) indicated a high degree of spatial variation in plant cover at the plot to canopy scale. The average heights of tree and herbaceous canopies were 2.7 m and 0.7 m, respectively. Measured profiles of root

abundance for grasses and broad-leaved trees indicated a greater abundance of roots in the upper soil for grasses, with tree root densities more constant with depth (most likely continuing well below the observation depth, which was limited in these sands by trench stability concerns) (Figure 1).

4.2. Rainfall Event and Soil Moisture

[15] An 85-mm rainfall event, recorded in a rain gauge within 3 km of the sites, occurred over two days in early March 2002, day of year (DOY) 66 and 67, followed by 30 days free of additional rain at the tower sites (this period is hereinafter referred to as the drydown). At the grass site, soil moisture ranged from 0.28 to 0.06 at 15 cm below the surface, $\theta(15)$, indicating a wide range of soil moisture conditions experienced by vegetation through the drydown (Figure 2). The soil moisture at the mixed site was less than that at the grass site, ranging only from 0.11 to 0.09 at 15 cm below the surface, potentially because of less local rainfall due to the convective nature of storms in the region, or more rapid drainage, which could be linked to greater macropore flow, coarser soils, or less organic matter.

4.3. Diurnal and Daily Energy and Mass Fluxes

[16] Soil drying following the rain event significantly affected energy, water, and carbon exchanges, as indicated by diurnal courses of H, LE, and Fc as shown in Figure 3 for two cloudless days, one wet (DOY 75), 8 days after the rain event, and one dry (DOY 95), 28 days after the rain, where wet and dry refer to the relative water status of the soil. Soil moisture at 15-cm depth decreased by 46% at the
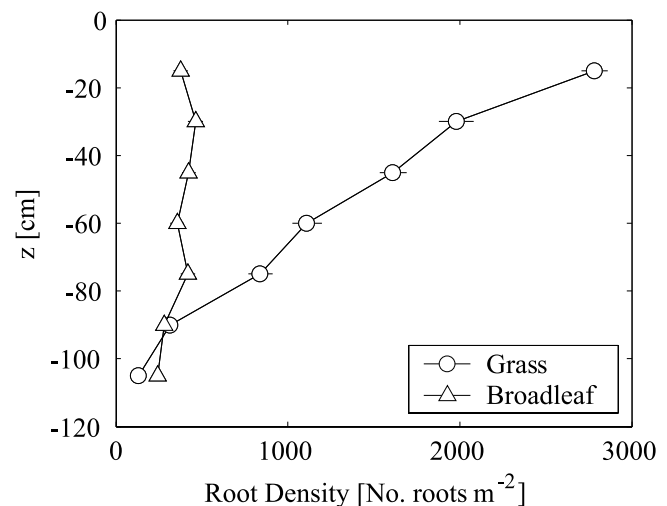

Figure 1. Root density profiles for broadleaf and grass functional types. Horizontal lines indicate standard deviation.
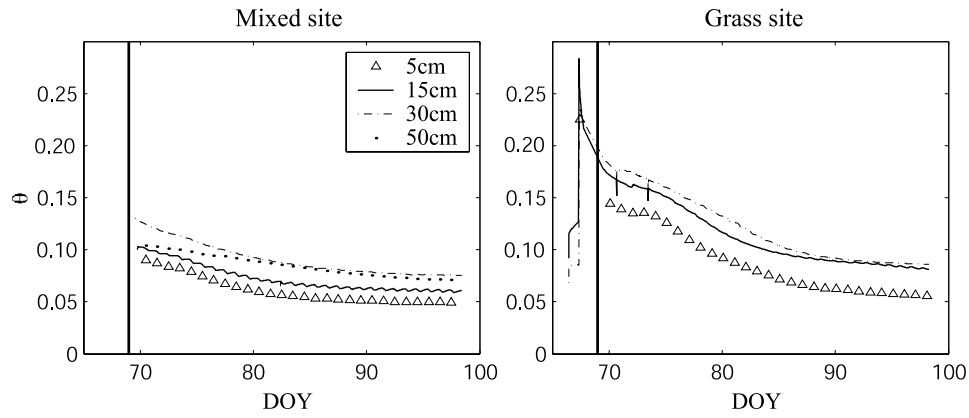
Figure 2. Volumetric soil water content as a function of day of year at the grass and mixed sites for depths 5, 15, 30, and 50 cm below the soil surface. The solid vertical bar illustrates the day (DOY 69) on which eddy covariance measurements began.

grass site and 32% at the mixed site between days 75 and 95 (Figure 2).

[17] To elucidate day-to-day, rather than diurnal, trends, we calculated mean daytime values from the average of observations between 0900 and 1600 hours (denoted throughout with angle brackets) (Figure 4). We analyzed the sensitivity of day-to-day trends to the hours that were included in daytime averaging by comparing results obtained from averaging over 0700 and 2000 hours with those from averaging over 0900 and 1600 hours, and the mean daytime water vapor and CO_2 fluxes were not significantly altered and their responses to environmental controls were identical. $\langle Rn \rangle$ was less than 300 W m^{-2} for the first three full days of observation, DOY 70–72, because of cloud cover,
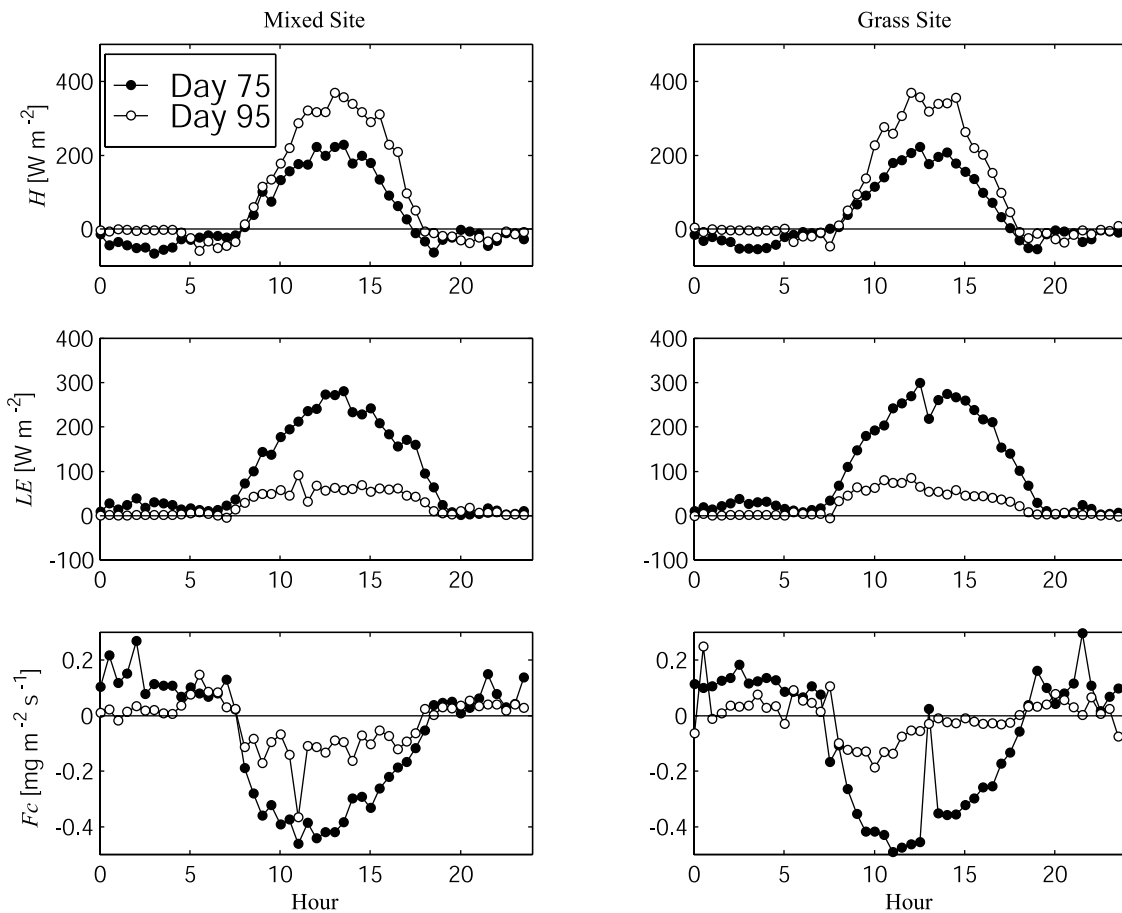

Figure 3. Diurnal courses of half-hourly H, LE, and Fc at the mixed and grass sites for two representative days during the drydown, where day 75 had relatively high soil water content in the surface soils and day 95 had low soil water content in the surface soils.
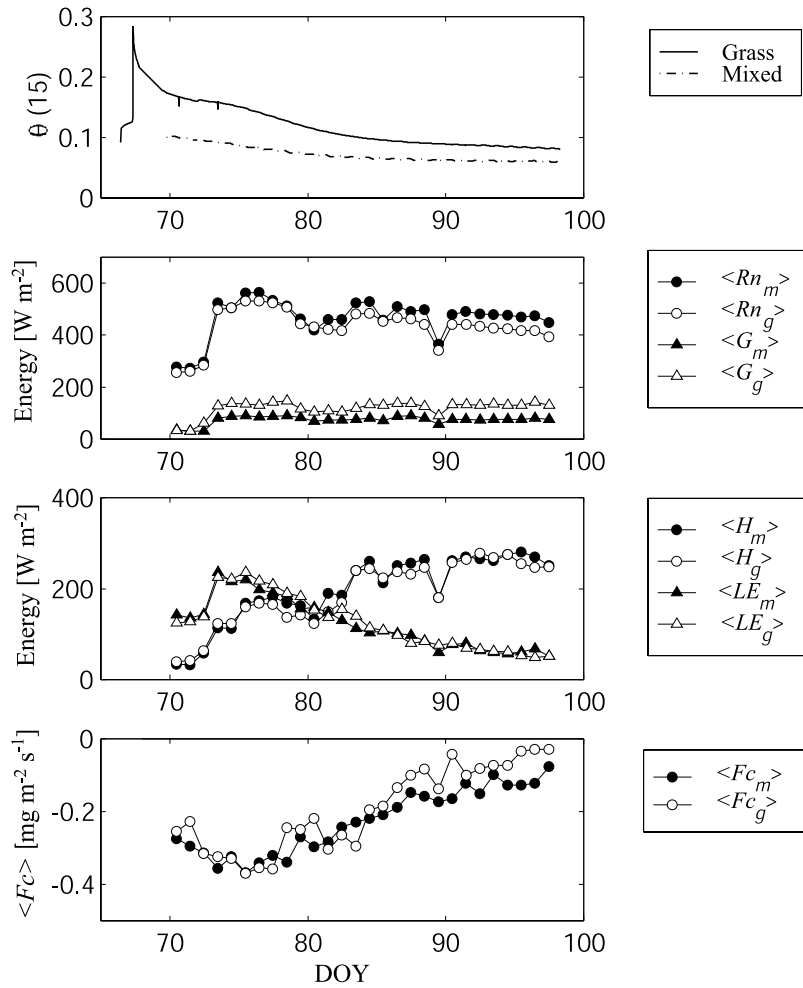
Figure 4. Soil moisture at 15-cm depth, and $\langle Rn \rangle$, $\langle G \rangle$, $\langle H \rangle$, $\langle LE \rangle$, and $\langle Fc \rangle$ at the grass (open) and mixed (closed) sites through the drydown experiment.

increased after DOY 72, and then exhibited a gradual decrease from DOY 73 to the end of the drydown experiment associated with a temporal increase in surface temperatures (Figure 4). Higher $\langle Rn \rangle$ and lower $\langle G \rangle$ at the mixed site as compared with the grass site resulted in approximately 80 W m^{-2} more available energy at the mixed site. The absence of strong trends in $\langle T_a \rangle$, $\langle Rn \rangle$, and $\langle u \rangle$ (Figures 4 and 5) is consistent with the assumption that the major dynamics in $\langle H \rangle$, $\langle LE \rangle$, and $\langle Fc \rangle$ during the drydown can be attributed largely to the consistent trends in soil moisture (Figures 2 and 4), and potentially an increased vapor pressure deficit (VPD, kPa) as demonstrated by the decreased $\langle q_a \rangle$ and increased mean daytime saturated specific humidity, $\langle q^* \rangle$ [g water vapor kg^{-1} moist air] (Figures 5 and 6).

[18] The decreases in $\langle LE_g \rangle$, and $\langle LE_m \rangle$ over the drydown (Figure 4) correspond to a decline in total daily evapotranspiration, ET_{daily} [mm d^{-1}], from approximately 2.8 to 0.7 mm d^{-1}. *Hutley et al.* [2001] reported a similar range in ET_{daily} from a wet season maximum of about 3.5 mm d^{-1} to values as low as 0.3 mm d^{-1} during the dry season for a site in northern Australia receiving approximately 520 mm of rain annually. Corresponding to the decrease in ET_{daily} over the drydown reported here, minimum daily Fc (maximum rate of CO$_2$ uptake by the land surface in a day) was approximately -0.5 mg CO$_2$ m^{-2} s^{-1} in the early part of the
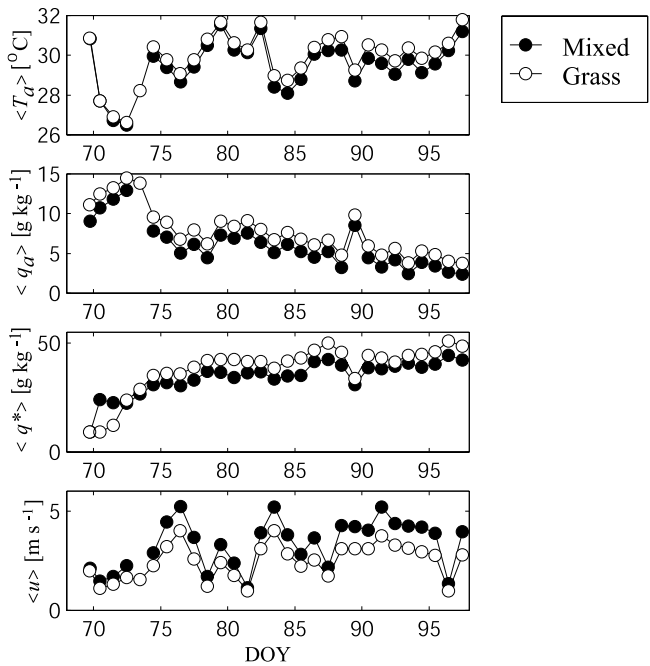

Figure 5. Environmental conditions during the drydown at the mixed and grass sites including $\langle T_a \rangle$, $\langle q_a \rangle$, $\langle q^* \rangle$, and $\langle u \rangle$.
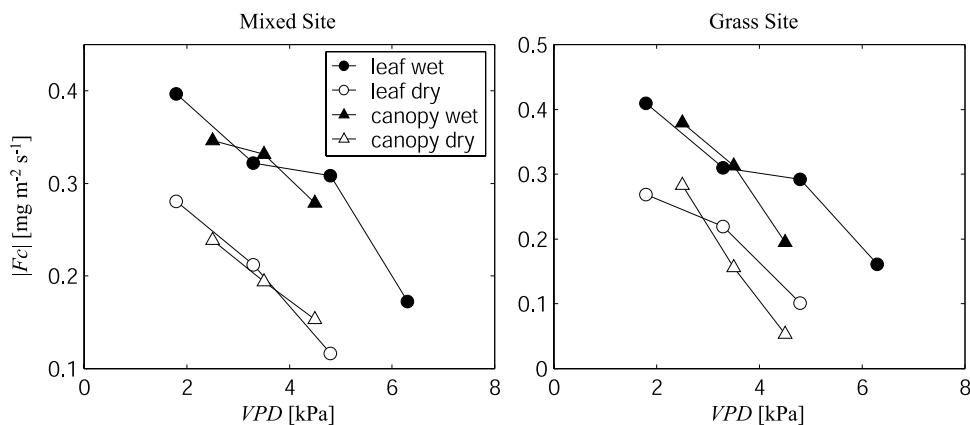
Figure 6. Leaf-scale (leaf) estimates and canopy-scale (canopy) measurements of Fc as a function VPD for light-saturated observations (photosynthetically active radiation >1000 μmol m^{-2} s^{-1}) binned by VPD for measurements taken during the wet and dry periods.

drydown, and this dampened to -0.1 mg CO_2 m^{-2} s^{-1} by the end of the drydown experiment (data not shown). The range in minimum daily Fc we observed was similar to that reported by *Verhoef et al.* [1996], -0.44 to -0.17 mg CO_2 m^{-2} s^{-1}, for observations during a 3-week wet-to-dry season transition of the HAPEX-Sahel experiment, as well as results from *Eamus et al.* [2001], who documented wet to dry season variation in minimum daily Fc of -0.48 to -0.09 mg CO_2 m^{-2} s^{-1} for a *Eucalyptus*-dominated savanna in Northern Australia. Correspondence between the ranges of water and carbon exchanges reported here with those reported from seasonal experiments suggests that the environmental conditions during the month-long drydown documented here were characteristic of a land surface response to seasonal changes in water availability affecting savanna water use and productivity.

4.4. Leaf-Scale Observations

[19] Simplified models of vegetation-atmosphere exchange of mass and energy typically assume linear scaling with leaf area index to estimate fluxes at larger scales. We compared leaf-scale gas exchange measurements with canopy-scale eddy covariance flux measurements to investigate this leaf-to-canopy scaling assumption. In addition to examining leaf-to-canopy scaling, we investigated how soil moisture limitation altered the responses of leaf- and canopy-scale CO_2 exchanges to VPD.

[20] Observations of leaf-scale gas exchange (H$_2$O and CO_2) were made on four species including two broad-leaved deciduous trees, a fine-leaved *Acacia*, and a representative and abundant C4 grass. Sampling logistics limited us to only 4 days of observations, so we pooled the data into wet and dry periods, where the wet period included observations made on days 77 and 81 and the dry period included observations made on days 84 and 87. Rn, T_a, q_a, $qz$and u were similar for the wet and dry periods (Figures 4 and 5). In contrast, soil moisture in the upper 40 cm of soil, $\theta(0-40)$, decreased from the wet to dry periods by ~0.02 at the mixed site and ~0.04 at the grass site, where $\theta(0-40)$ was calculated from a depth-weighted average of θ measurements at 5, 15, and 30 cm, representing zones of $0-10$, $10-22.5$, and $22.5-40$ cm below the surface, respectively. We studied how soil moisture reduction from

the wet to dry period altered the response of both leaf- and canopy-scale CO_2 exchange to VPD, where leaf-scale observations were rescaled to provide estimates of canopy-scale CO_2 exchange. Leaf-scale observations were rescaled to a canopy-scale by neglecting nonleaf respiration and multiplying A by the appropriate LAI_{veg} of grass or tree canopies and by their respective fractional covers at the mixed and grass sites (Tables 2 and 3), using the dominant tree, *Acacia*, to represent contributions from woody vegetation. For analysis of leaf-scale observations, VPD was computed from chamber-based measurements of leaf temperature and air specific humidity, while tower-based air temperature and specific humidity were used to compute VPD for analysis of canopy-scale fluxes.

[21] The piecewise linear soil moisture limitation function of equation (2) can be used to obtain an expectation of the change in CO_2 exchange for the observed changes in soil moisture. Applying equation (2) with critical and wilting-point soil moisture parameters appropriate for grass and woody savanna vegetation (see section 4.6, where grass $\theta_{cr} = 0.18$, $\theta_{wilt} = 0.05$; woody $\theta_{cr} = 0.11$, $\theta_{wilt} = 0.05$), we estimated the decrease in ET_{daily} that would be expected due to the observed decreases in soil moisture from the wet to dry periods. The change in $\theta(0-40)$ from 0.10 to 0.08 at the mixed site is 33% of the range in soil moisture from the critical point to the wilting point (0.11 to 0.05). Since $\theta(0-40)$ was less than θ_{cr} and greater than θ_{wilt} for the wet and dry periods, we would anticipate a ~30% decrease in ET_{daily} over the wet to dry period at the mixed site. A similar calculation for the grass site indicates that the 0.04 decrease in $\theta(0-40)$ is expected to result in a similar ~30% decrease in ET_{daily} over the wet to dry period. Assuming a constant daytime WUE over the wet to dry period, we would expect a ~30% decrease in $|Fc|$ at the two sites between the wet and dry periods.

[22] When scaled by LAI_{veg} and aggregated by fractional cover components, the observations at the leaf-scale matched well those at the canopy scale for both the mixed and grass sites (Figure 6). Furthermore, for a given VPD, $|Fc|$ decreased by approximately $30-35$% from the wet to the dry period (Figure 6), which is consistent with an expected ~30% reduction in $|Fc|$ at both sites. Good agreement between canopy- and leaf-scale observations
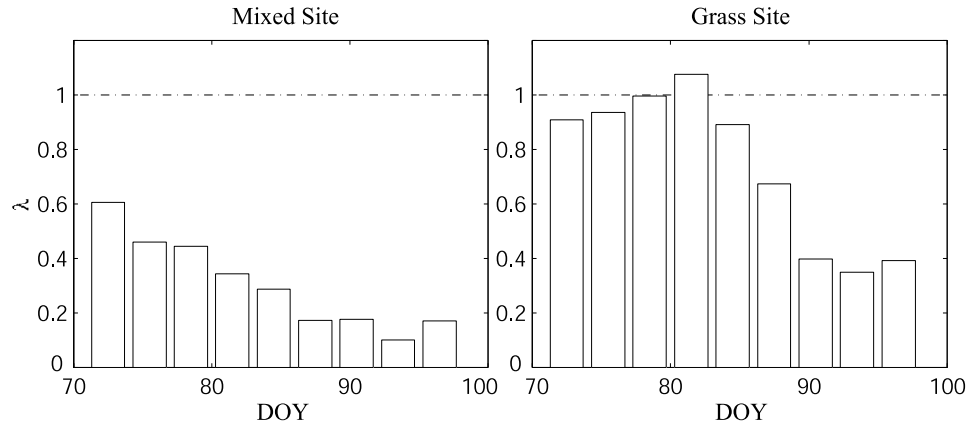
Figure 7. The fraction of measured ET_{daily} that can be accounted for by the mass balance of soil water in the upper soil (λ) at the mixed and grass sites binned into 3-day averages.

suggests that modeling leaf-scale ecophysiological processes may provide reliable estimates of canopy-scale exchanges when rescaled linearly by vegetation density as suggested elsewhere by *Norman* [1993] and *Scholes and Walker* [1993]. In addition, the results are consistent with the expectation that during the daytime, soil fluxes of water and carbon were small relative to plant exchanges. At first glance, the agreement between rescaled leaf photosynthesis and $\langle Fc \rangle$ appears counterintuitive because of respiration. In section 4.9 we provide plausible arguments that leaf respiration is a significant fraction of ecosystem respiration, and though negligible during daytime, it can be a large fraction of nighttime ecosystem CO_2 fluxes.

4.5. Inferred Root Water Uptake

[23] Having introduced the general drydown response of mass and energy exchanges, we study how the drydown influenced root water uptake in the near-surface rooting zone. With this analysis we investigated whether plant water uptake tended to be deeper at the site with more trees (mixed) and, furthermore, how the profile of water extraction behaved through the drying. We estimated the fraction of daily evapotranspiration contributed by soil moisture stored in the upper 40 cm of soil based on measured changes in soil moisture at 5-, 15-, and 30-cm depths. In the absence of rainfall inputs, and ignoring horizontal flow on this relatively flat terrain, the change in soil moisture is due to evaporation, root water uptake, or a vertical flux of water across the bottom boundary of the 40-cm-deep soil profile. Using Darcy's law between 5- and 15-cm depths to estimate the delivery of water to the evaporating surface, and between 15- and 30-cm depths to estimate water flux across the bottom boundary, we calculated soil water fluxes more than an order of magnitude less than ET_{daily} for the entire drydown at the mixed site, and after DOY 78 at the grass site. These estimates suggest that bare soil evaporation and vertical water flux were negligible soon after the rain event and that nearly all of the ET_{daily} toward the middle to end of the drydown can be attributed to root water uptake.

[24] The ratio of ET_{daily} estimated from the mass balance of soil moisture to ET_{daily} measured with eddy covariance provides an estimate of the fraction of ET_{daily} contributed by the upper 40 cm of soil, represented here by λ (Figure 7). At the grass site, nearly all of ET_{daily} was contributed from the

upper 40 cm of soil ($\lambda \sim 1$) for the first $\sim$15 days of drying, followed by a decline in λ. After 30 days of drying, only $\sim$40% of the ET_{daily} was contributed by the upper 40 cm of soil, as the center of mass for root water uptake by grass deepened with time since rainfall. At the mixed site, λ was about 0.65 three days after the rain event, and less than 0.2 after 30 days of drying (Figure 7). The relatively low λ at the mixed site in comparison with the grass site immediately following the rain event indicates that the deeper portion of the root zone of vegetation at the mixed site was active even in wet conditions and became even more active as the surface dried. The results show a continued deepening of the center of mass of root water uptake in the presence of continued drying for both sites. These findings are consistent with other studies that show that plants can preferentially extract water from near-surface soils when water is abundant but are able to respond to near-surface soil drought by extracting water from deeper in the soil profile [*Green and Clothier*, 1995; *Huang et al.*, 1997; *Lai and Katul*, 2000; *Li et al.*, 2001, 2002].

4.6. Soil Moisture Limitation of ET

[25] To evaluate the skill of equation (2), we estimated β with measurements of f_v and half-hourly ET and PET, as in equation (1). Figure 8 compares estimates of mean daytime (900–1600 hours) β, $\langle\beta\rangle$, as a function of the soil moisture in the upper $\sim$40 cm of the root zone, $\theta(0-40)$. We also plot here the piecewise linear soil moisture limitation function of equation (2) with the critical and wilting-point parameters obtained from literature values of trees and grasses representative of those present in the respective tower footprints. *Scholes and Walker* [1993] report critical and wilting-point soil water potentials of -0.29 and -3.9 MPa for *Eragrostis pallens* and -0.24 and -1.9 MPa for *Terminalia sericea*, and -0.71 and -3.1 MPa for *Burkea africana*, a woody plant similar in function to *Acacia* and used for the critical soil water of *Acacia*. Numerous authors report minimum *Acacia* leaf water potentials between -2.0 and -3.5 MPa [*Hesla et al.*, 1985; *Eamus and Cole*, 1997; *Liang et al.*, 1997], and in severe drought conditions, *Acacia* predawn xylem water potential can be as low as -6.8 MPa [*Tunstall and Connor*, 1981]. While leaf and xylem water potentials are lower than soil water potentials for $ET > 0$, they
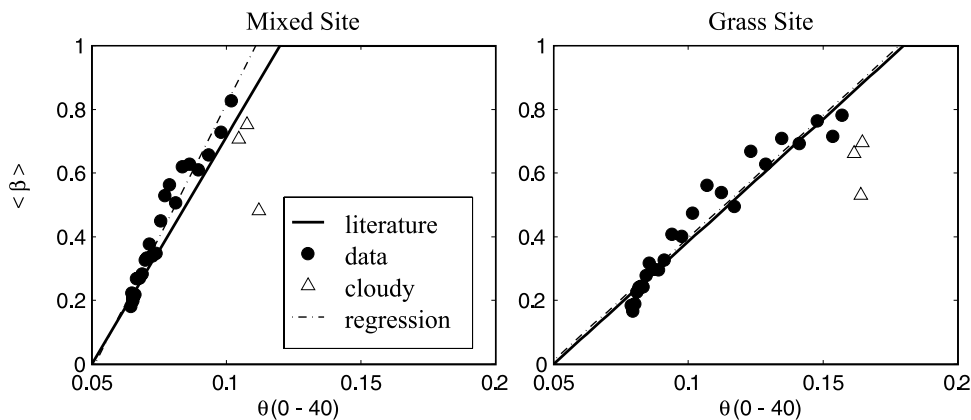
Figure 8. Estimated $\langle\beta\rangle$ as a function of θ averaged from measurements at 5-, 15-, and 30-cm depths, $\theta(0-40)$, plotted with the piecewise linear soil moisture limitation function using literature values of the critical and wilting point parameters, as well as the linear regression of $\langle\beta\rangle$ on θ, omitting observations taken on cloudy days.

provide an indication of the critical and wilting-point soil water potentials that could be appropriate for use in equation (2). These water potentials for *Eragrostis*, *Terminalia*, and *Acacia* correspond to θ_{cr} of 0.18, 0.19, and 0.08, and to θ_{wilt} of 0.05, 0.06, and 0.05, respectively. The *Eragrostis* parameters were used alone for the grass site data, and the average of *Eragrostis* and *Acacia* parameters were applied for the mixed site, yielding θ_{cr} of 0.12 and θ_{wilt} of 0.05.

[26] Estimates of $\langle\beta\rangle$ matched well the prediction with equation (2) over a wide range of soil moisture, indicating robustness of the piecewise linear approximation (Figure 8). Days with cloudy, humid, low-wind-speed conditions were excluded from regression analysis, as α was less than 1.26. Threshold breakpoints determined from the data ($\theta_{cr} = 0.18$ and $\theta_{wilt} = 0.05$ at the grass site, and $\theta_{cr} = 0.11$ and $\theta_{wilt} = 0.05$ at the mixed site) were close to those reported in the literature.

4.7. Analytical Models of *ET* Decay With Time Since Rainfall

[27] One alternative to modeling ET_{daily} as a function of daily environmental conditions is to characterize the structure of ET_{daily} as a function of time since a wetting event. We tested the ability of the two-stage model, described in section 2.2, to capture the decay rate of ET for a vegetated surface. Figure 9 compares the measured ET_{daily} at the mixed and grass sites with the second stage model, indicating that the decay of ET_{daily} for the vegetated surface was slower than that predicted for desorption of a bare soil surface ($t^{-1/2}$). The desorption process responsible for decay of E is mechanistically very different from the process of soil moisture limitation causing T decay in time. Soil moisture desorption is structured by the rate of delivery of soil moisture at depth to the evaporating surface of the soil. In contrast, plants have prolonged access to soil water resources through their distributed hydraulic network of roots that adapts water acquisition to acquire water from wetted zones as soil moisture availability evolves in space and time [*Li et al.*, 2001, 2002]. The results we present are consistent with the expectation of more gradual decay of transpiration with time since a wetting event as compared with the theoretical decay of bare soil evaporation.

[28] Another simple approach for estimating the time rate of change of daily evapotranspiration (dET_{daily}/dt) can be obtained from a combination of equations (1) and (2) and
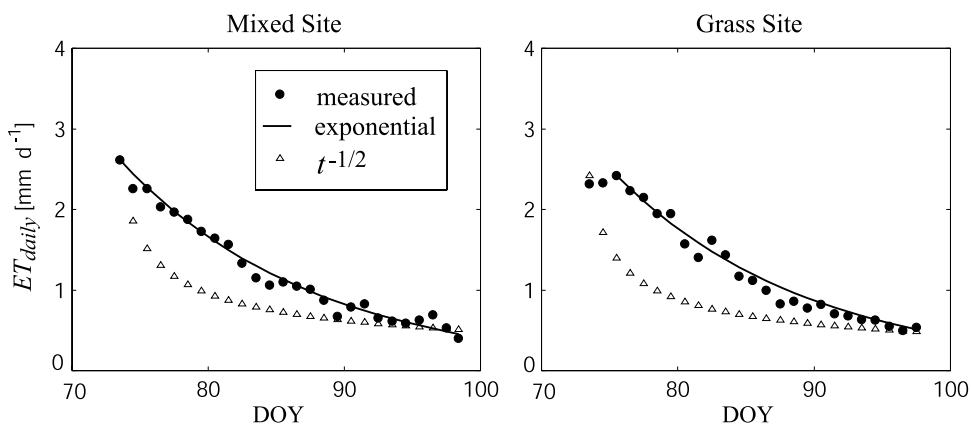

Figure 9. Decay of ET_{daily} measured and modeled with the exponential model equation (9), and $t^{-1/2}$ presented as a reference to the theoretical decay from soil desorption.
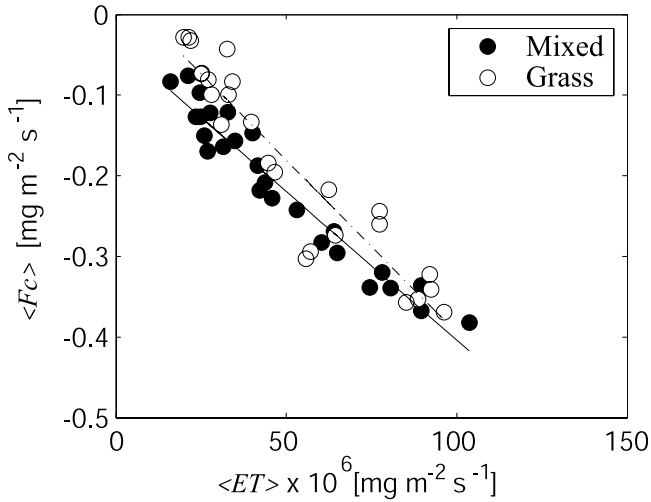
Figure 10. $\langle Fc \rangle$ versus $\langle ET \rangle$ at the grass (open symbols) and mixed sites (closed symbols). Regression lines are also shown for the mixed (solid) and grass (dashed) sites.

adopting the assumptions outlined in section 4.5. First we apply the chain rule to dET_{daily}/dt to obtain

$$\frac{\mathrm{d}ET_{daily}}{\mathrm{d}t} = \frac{\partial ET_{daily}}{\partial \theta} \frac{\partial \theta}{\partial t}. \tag{6}$$

Assuming that the change in rooting zone soil moisture with time for a rooting zone of depth d is balanced by evapotranspiration in the absence of rainfall or soil water flux, allows the substitution of $-ET_{daily}/d$ into equation (6), as

$$\frac{\mathrm{d}ET_{daily}}{\mathrm{d}t} = \frac{\partial ET_{daily}}{\partial \theta} \frac{ET_{daily}}{d}. \tag{7}$$

Substituting equation (1) into (7) for the range $\theta_{wilt} \leq \theta \leq \theta_{cr}$ (as appears to represent most conditions in these coarse soils), and assuming that total daily PET, PET_{daily}, is constant in time, yields

$$\frac{\mathrm{d}ET_{daily}}{\mathrm{d}t} = -\frac{ET_{daily}\left(PET_{daily}f_v\right)}{d(\theta_{cr} - \theta_{wilt})}. \tag{8}$$

Integrating equation (10) with respect to time yields an exponential decay, as

$$ET_{daily}(t) = ET_o \exp\left[-\frac{PET_{daily}f_v\hat{t}}{d(\theta_{cr} - \theta_{wilt})}\right], \tag{9}$$

where ET_o is the initial daily rate following the rain event and $\hat{t}$ is the time (days) since rainfall.

[29] The above result shows that the soil moisture limitation function for $\theta_{wilt} \leq \theta \leq \theta_{cr}$ yields a two-parameter analytical model with an exponential decay of evapotranspiration. The hydraulic properties of the coarse soils and semiarid climate cause θ to be below θ_{cr} and above θ_{wilt} during most of the growing season for much of the Kalahari region of southern Africa, enabling us to safely adopt the assumptions implicit to equation (9). We applied

the analytical model described by equation (9), defining ET_o from the maximum of the observed ET_{daily} at each site, using the critical and wilting-point soil moisture parameters determined above (section 4.6), and determining d by fitting estimates of ET_{daily} with equation (9) to the measured ET_{daily}, yielding 0.4 m for the grass site and 0.8 m for the mixed site.

[30] The exponential model of equation (9) provides an excellent fit to the data at the grass ($R^2 = 0.92$) and mixed ($R^2 = 0.92$) sites for the extended period of drying (Figure 9). By applying a constant PET_{daily} throughout drydown, equation (9) assumes that environmental state variables such as Rn, T_a, and q_a are sufficiently stationary for the entire interstorm period, but the additional complication of time-varying environmental conditions, in addition to soil moisture, could be easily considered in a numerical application of equation (9).

4.8. Water Use Efficiency

[31] At a daily time step, we average out the diurnal or daytime fluctuations in WUE to more clearly identify potential changes in WUE as the surface dried. Figure 10 shows $\langle Fc \rangle$ versus $\langle ET \rangle$ over the drydown, revealing strong correlation at the mixed ($R^2 = 0.94$) and grass ($R^2 = 0.90$) sites with a linear relationship capturing much of the variability. The intercept of the regression was positive for the grass site but negative for the mixed site (Table 4), and the slopes were not statistically different between sites ($P > 0.05$), suggesting that respiration was greater at the grass site than at the mixed site. The linear relationship between $\langle Fc \rangle$ and $\langle ET \rangle$ indicates that $\langle WUE \rangle$ varied little throughout the drydown, with approximately -0.005 kg CO_2 per kg H_2O. This is consistent with the findings of *Verhoef et al.* [1996], who reported less than 10% variation in $\langle Fc \rangle / \langle ET \rangle$ for days with high versus low soil moisture. Next, we evaluate the goodness of fit between measured $\langle Fc \rangle$ and that estimated from modeled $\langle ET \rangle$ coupled with the empirically derived constant $\langle WUE \rangle$.

4.9. Analytical Prediction of Carbon Exchange

[32] Mechanistic coupling and strong correlation between ecosystem water and carbon exchanges with the atmosphere suggest that carbon uptake should decay at a rate similar to that found for evapotranspiration. We compared measured $\langle Fc \rangle$ over the drydown with that predicted from $\langle ET \rangle$ modeled with equation (1), represented as ET^*, multiplied by the empirically derived $\langle WUE \rangle$. We obtained a good approximation to the data with this simple modeling approach, with R^2 of 0.95 and 0.86 for the mixed and grass sites, respectively (Figure 11). These results suggest that a constant daily WUE may be adequate for obtaining $\langle Fc \rangle$ from $\langle ET \rangle$.

[33] This analysis primarily deals with determining $\langle Fc \rangle$ from $\langle ET \rangle$, so its utility is limited by variability in $\langle ET \rangle$. At night, ET approaches zero, while Fc approaches ecosystem

Table 4. Regression Parameters From $\langle Fc \rangle$ Versus $\langle ET \rangle$ With P Values in Parentheses

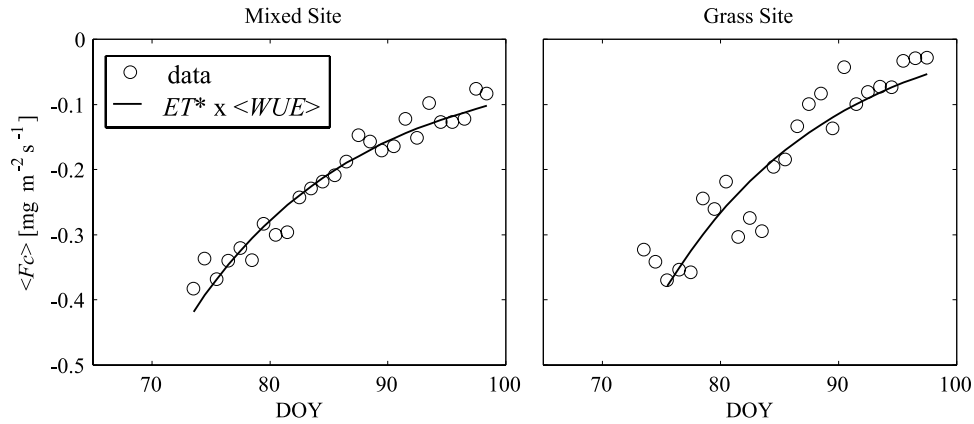| Site	Slope	Intercept	R^2
Grass	-0.0042 (<0.001)	0.034 (0.002)	0.90
Mixed	-0.0037 (<0.001)	-0.036 (0.058)	0.94

Figure 11. Decay of $\langle Fc \rangle$ from observations (data) and modeled with equation (9) multiplied by the empirically derived $\langle WUE \rangle$ at the mixed and grass sites.

respiration, for which soil moisture may be a significant control (Figure 3). Therefore, to extrapolate this work to total daily net CO_2 exchange, Fc_{daily} [mg m^{-2} d^{-1}], we need to account for nighttime respiration in the daily carbon balance. To investigate the role of nighttime respiration in the savanna carbon balance over the drydown, we examined Fc between the nighttime hours of 2200 and 0500 LST. Because eddy covariance flux measurements may not represent well ecosystem respiration for stable atmospheric conditions, we excluded Fc observations in this analysis if the friction velocity ($u*$) was less than 0.1 m s^{-1}, the minimum threshold of those typically selected [*Baldocchi*, 2003]. That is, with this $u*$ threshold, the flow approaches near-neutral conditions and the fluxes are better coupled to the biological sources and sinks [*Cava et al.*, 2004]. In addition, we examined 3-day average fluxes and states, denoted as $\langle \rangle_{3day}$ to elucidate trends over the drydown in spite of large variability in half-hourly fluxes.

[34] Nighttime $\langle Fc \rangle_{3day}$ declined as much as 40% over the drydown and was positively related to soil moisture at the mixed ($R^2 = 0.76$) and grass ($R^2 = 0.61$) sites (Figure 12), consistent with a growing body of evidence that suggests soil moisture is an important control on ecosystem respiration, particularly in water-limited ecosystems [*Wildung et al.*, 1975; *Mielnick and Dugas*, 2000; *Liu et al.*, 2002]. Hence the reduction in daytime CO_2 flux with decreasing soil moisture was matched by a proportional reduction in respiration. To illustrate, we found that the nighttime $\langle Fc \rangle_{3day}$ decayed with a temporal structure similar to that for daytime $\langle Fc \rangle_{3day}$, as evidenced by the relatively steady absolute value of the ratio of nighttime to daytime $\langle Fc \rangle_{3day}$, denoted as μ, which ranged between 0.29 and 0.47 for nearly the entire drydown period (Figure 12). This result permits estimation of Fc_{daily} from ET_{daily} and WUE, as

$$Fc_{daily} = \langle Fc \rangle + \langle\langle Fc \rangle\rangle = WUE \times ET_{daily} - \langle\langle Fc \rangle\rangle$$

$$\langle\langle Fc \rangle\rangle = \mu(\theta) \times \langle Fc \rangle \qquad , \quad (10)$$

where $\langle\langle Fc \rangle\rangle$ is nighttime Fc, daytime CO_2 flux is relative to $ET > 0$, and daytime and nighttime periods each occupied 12 hours per day, as evident in Figure 3. After ~16 days of drying (DOY > 86) at the grass site only, μ increased, suggesting that the contribution of respiration to

total daily CO_2 flux increased relative to $\langle Fc \rangle$. We note that this model may not be entirely general because as $ET_{daily} \rightarrow 0$ after a prolonged drought, $Fc_{daily} \rightarrow 0$, which is not entirely correct because a finite respiring biomass still exists.

[35] An apparent contradiction arises between the finding that nighttime Fc was ~40% as large as daytime Fc, and the finding (section 4.4) that respiration was a small fraction of daytime CO_2 exchange. This apparent inconsistency can be resolved by considering that leaf respiration may be a large fraction of nighttime ecosystem CO_2 exchange, but is negligible during the daytime when net assimilation dominates measured exchanges. A first approximation of the lower limit of nighttime leaf respiration rate can be obtained by estimating dark respiration rate, Rd [mg m^{-2} s^{-1}], as 0.015 times the maximum Rubisco capacity, V_{cmax}, [mg m^{-2} s^{-1}] [*Campbell and Norman*, 1998]. V_{cmax} was estimated from the temperature response for Kalahari vegetation reported by *Midgley et al.* [2004], providing a range corresponding to typical leaf temperatures for nighttime conditions during the drydown experiment (25°C). We obtained V_{cmax} of 3.3–5.5 mg m^{-2} s^{-1} and Rd of 0.049–0.083 mg m^{-2} s^{-1}, which could contribute as much as 60% of the maximum nighttime $\langle Fc \rangle_{3day}$ (0.14 mg m^{-2} s^{-1}) (Figure 12). This estimate confirms that plant respiration could have contributed a large fraction of nighttime ecosystem CO_2 exchange, and is consistent with the relatively steady μ, as both nighttime and daytime CO_2 exchanges are coupled to V_{cmax}.

5. Conclusions

[36] The results presented in this study support prevailing theories of savanna water and carbon functional responses to changes in soil moisture applied in ecohydrological modeling of savannas. A common piecewise linear function characterizing soil moisture limitation of ET_{daily} was in good agreement with the data and literature values for critical and wilting-point parameters. The deterministic decay of ET_{daily} was well captured by an analytical exponential model obtained from PET_{daily} and the soil moisture limitation function of equation (2), enabling a storm-scale approach whereby we could predict temporal dynamics of plant water use and soil moisture by estimating
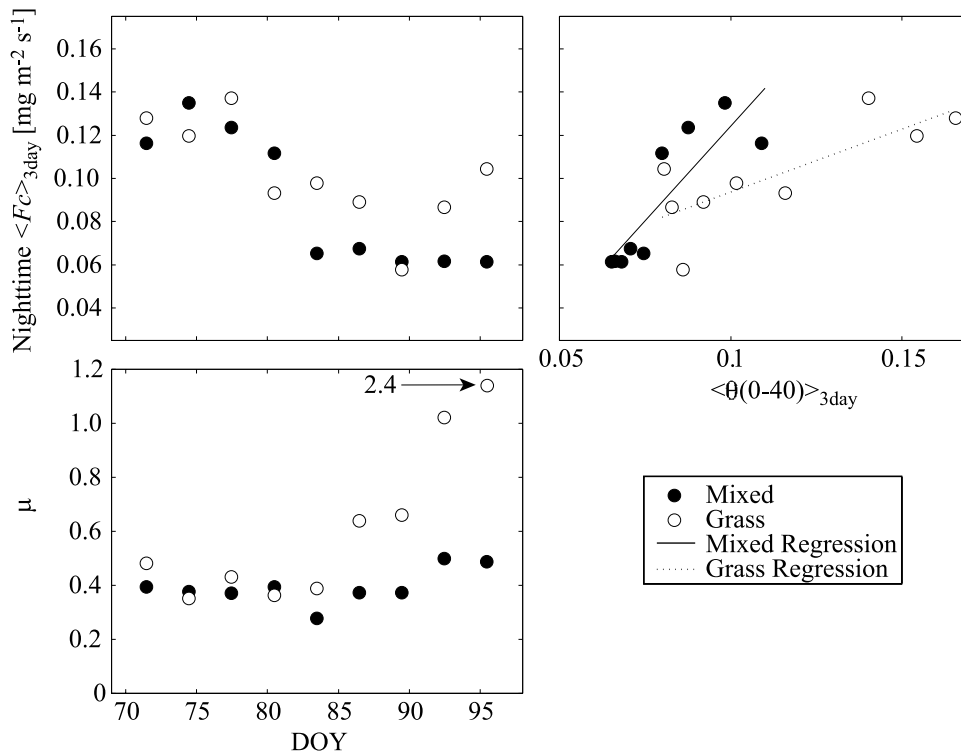
Figure 12. Three-day mean Fc for nighttime observations over time and versus 3-day mean $\langle\theta(0-40)\rangle_{3day}$, and the ratio of nighttime to daytime 3-day mean $|Fc|$, μ, at the mixed and grass sites over the drydown period.

the initial conditions of PET_{daily} and ET_o with initial soil moisture conditions updated for each rain event, and then applying equation (9) as an interstorm decay. Canopy-scale measurements of water and carbon exchanges confirmed that water use efficiency provides reasonable estimates of CO_2 uptake based on knowledge of vegetation water use at the daily timescale.

[37] Taken together, these results motivate a simplified approach to modeling ecosystem water and carbon exchanges by focusing on the water limitation of transpiration defined by critical and wilting-point parameters and time since rainfall. The simplifying assumptions supported by our findings suggest that the complex dynamics of water-limited ecosystems can be reduced with a modeling scheme that preserves the most important features of savanna function. The probabilistic approach outlined by *Rodriguez-Iturbe et al.* [2001] is well suited for studying water and carbon fluxes as deterministic, interstorm processes dependent on the stochastic nature of storm arrivals and depths. Provided the statistical structure of storm depth and interarrival, we could use the analytical model of equation (9) to provide ET_{daily} as a function of initial soil moisture following a rain event and use a mean daytime WUE and μ to provide total daily CO_2 exchange as in equation (10). Integration of plant carbon balance through time would allow vegetation structure to be updated, feeding back on ecosystem function (ET and Fc) through changes in vegetation cover and leaf area. The fundamental processes of water-limited savannas described here provide important building blocks for studying climate sensitivity of savanna function (e.g., ET, Fc) and structure (e.g., LAI, f_v) and may be useful for investigating the resilience and stability of the tree-grass mixture with respect to perturbations in environmental conditions.

References

Albertson, J. D., and G. Kiely (2001), On the structure of soil moisture time series in the context of land surface models, *J. Hydrol.*, *243*, 101–119.

Atjay, G. L., P. Ketner, and P. Duvigneaud (1979), Terrestrial primary production and phytomass, in *The Global Carbon Cycle: SCOPE 13*, edited by B. Bolin et al., pp. 129–182, John Wiley, Hoboken, N. J.

Avissar, R., and R. A. Pielke (1991), The impact of plant stomatal control on mesoscale atmospheric circulations, *Agric. For. Meteorol.*, *54*, 353–372.

Baillieul, T. A. (1975), A reconnaissance survey of the cover sands in the Republic of Botswana, *J. Sediment. Petrol.*, *45*, 495–503.

Baldocchi, D. D. (2003), Assessing the eddy covariance technique for evaluating carbon dioxide exchange rates of ecosystems: Past, present and future, *Global Change Biol.*, *9*, 479–492.

Bruce, R. R., and A. Klute (1956), The measurement of soil moisture diffusivity, *Soil Sci. Soc. Am. Proc.*, *20*, 458–462.

Brutsaert, W. (Ed.) (1982), *Evaporation Into the Atmosphere: Theory, History, and Applications*, 1st ed., 299 pp., Kluwer Acad., Norwell, Mass.

Brutsaert, W., and D. Chen (1995), Desorption and the two stages of drying of natural tallgrass prairie, *Water Resour. Res.*, *31*(5), 1305–1313.

Brutsaert, W., and D. Chen (1996), Diurnal variation of surface fluxes during thorough drying (or severe drought) of natural prairie, *Water Resour. Res.*, *32*(7), 2013–2019.

Caldwell, M. M., and R. A. Virginia (1989), Root systems, in *Plant Physiological Ecology: Field Methods and Instrumentation*, edited by R. W. Pearcy et al., pp. 367–371, Chapman and Hall, New York.

Campbell, G. S., and J. M. Norman (Eds.) (1998), *An Introduction to Environmental Biophysics*, 2nd ed., 286 pp., Springer-Verlag, New York.

Cao, M., Q. Zhang, and H. H. Shugart (2001), Dynamic responses of African ecosystem carbon cycling to climate change, *Clim. Res.*, 17, 183–193.

Cava, D., U. Giostra, M. Siqueira, and G. Katul (2004), Organised motion and radiative perturbations in the nocturnal canopy sublayer above an even-aged pine forest, *Boundary Layer Meteorol.*, 112, 129–157.

Clapp, R., and G. Hornberger (1978), Empirical equations for some soil hydraulic properties, *Water Resour. Res.*, 14(4), 601–604.

Eamus, D., and S. Cole (1997), Diurnal and seasonal comparisons of assimilation, phyllode conductance and water potential, of three Acacia and one Eucalyptus species in the wet-dry tropics of Australia, *Aust. J. Bot.*, 45, 275–290.

Eamus, D., L. B. Hutley, and A. P. O'Grady (2001), Daily and seasonal patterns of carbon and water fluxes above a north Australian savanna, *Tree Physiol.*, 21, 977–988.

Federer, C. A. (1979), A soil-plant-atmosphere model for transpiration and availability of soil water, *Water Resour. Res.*, 15(3), 555–562.

Ferrar, P. J. (1980), Environmental control of gas exchange in some savanna woody species: 1. Controlled environment studies of Terminalia-Sericea and Grewia-Flavescens, *Oecologia*, 47, 204–212.

Fisher, M. J., I. M. Rao, M. A. Ayarza, C. E. Lascano, J. I. Sanz, R. J. Thomas, and R. R. Vera (1994), Carbon storage by introduced deep-rooted grasses in the South American savannas, *Nature*, 371, 236–238.

Gardner, W. R. (1959), Solutions of the flow equations for the drying of soils and other porous media, *Soil Sci. Soc. Am. Proc.*, 23, 183–187.

Green, S. R., and B. E. Clothier (1995), Root water uptake by kiwi fruit vines following partial wetting of the root zone, *Plant Soil*, 173, 317–328.

Gollan, T., N. C. Turner, and E. D. Schulze (1985), The responses of stomata and leaf gas exchange to vapor pressure deficits and soil water content: 3. In the sclerophyllous species Nerium oleander, *Oecologia*, 65, 356–362.

Hesla, B. I., H. L. Tieszen, and T. W. Boutton (1985), Seasonal water relations of savanna shrubs and grasses in Kenya, East Africa, *J. Arid Environ.*, 8, 15–31.

Huang, B., R. R. Duncan, and R. N. Carrow (1997), Drought-resistance mechanisms of seven warm-season turfgrasses under surface soil drying: II. Root aspects, *Crop Sci.*, 37, 1863–1869.

Hutley, L. B., A. P. O'Grady, and D. Eamus (2001), Monsoonal influences on evapotranspiration of savanna vegetation of northern Australia, *Oecologia*, 126, 434–443.

Jackson, R. B., J. L. Banner, E. G. Jobbagy, W. T. Pockman, and D. H. Wall (2002), Ecosystem carbon loss with woody plant invasion of grasslands, *Nature*, 418, 623–626.

Jacquemin, B., and J. Noilhan (1990), Sensitivity study and validation of a land surface parameterization using the HAPEX-MOBILHY data set, *Boundary Layer Meteorol.*, 52, 93–134.

Jeltsch, F., G. E. Weber, and V. Grimm (2000), Ecological buffering mechanisms in savannas: A unifying theory of long-term tree-grass coexistence, *Plant Ecol.*, 150, 161–171.

Jolly, W. M., and S. W. Running (2004), Effects of precipitation and soil water potential on drought deciduous phenology in the Kalahari, *Global Change Biol.*, 10, 303–308.

Jones, H. G. (Ed.) (1983), *Plants and Microclimate*, 323 pp., Cambridge Univ. Press, New York.

Kaimal, J. C., and J. J. Finnigan (1994), *Atmospheric Boundary Layer Flows*, Oxford Univ. Press, New York.

Lai, C.-T., and G. Katul (2000), The dynamic role of root-water uptake in coupling potential to actual transpiration, *Adv. Water Resour.*, 23, 427–439.

Laio, F., A. Porporato, L. Ridolfi, and I. Rodriguez-Iturbe (2001), Plants in water-controlled ecosystems: Active role in hydrologic processes and response to water stress: II. Probabilistic soil moisture dynamics, *Adv. Water Resour.*, 24, 707–723.

Larcher, W. (1995), *Physiological Plant Ecology*, 3rd ed., Springer-Verlag, New York.

Le Houerou, H. N., and C. H. Hoste (1977), Rangeland production and annual rainfall felations in the Mediterranean Basin and the African Sahelo-Sudanian Zone, *J. Range Manage.*, 30, 181–189.

Le Roux, X., and P. Mordelet (1995), Leaf and canopy CO_2 assimilation in a West African humid savanna during the early growing season, *J. Trop. Ecol.*, 11, 529–545.

Li, K. Y., R. De John, and J. B. Boisvert (2001), An exponential root-water-uptake model with water stress compensation, *J. Hydrol.*, 252, 189–204.

Li, Y., M. Fuchs, S. Cohen, Y. Cohen, and R. Wallach (2002), Water uptake profile response of corn to soil moisture depletion, *Plant Cell Environ.*, 25, 491–500.

Liang, J., J. Zhang, and M. H. Wong (1997), Can stomatal closure caused by xylem ABA explain the inhibition of leaf photosynthesis under soil drying?, *Photosynth. Res.*, 51, 149–159.

Liu, X., S. Wan, B. Su, D. Hui, and Y. Luo (2002), Response of soil CO_2 efflux to water manipulation in a tallgrass prairie ecosystem, *Plant Soil*, 240, 213–223.

Mahfouf, J. H., C. Ciret, A. Ducharne, P. Irannejad, J. Noilhan, Y. Shao, P. Thornton, L. Xue, and Z.-L. Yang (1996), Analysis of transpiration results from the RICE and PILPS Workshop, *Global Planet. Change*, 13, 73–88.

McNaughton, K. G., and P. G. Jarvis (1983), Predicting the effects of vegetation changes on transpiration and evaporation, in *Water Deficits and Plant Growth*, vol. VII, *Additional Woody Crop Plants*, edited by T. T. Kozlowski, pp. 1–47, Academic, San Diego, Calif.

McNaughton, K. G., and P. G. Jarvis (1991), Effects of spatial scale on stomatal control of transpiration, *Agric. For. Meteorol.*, 54, 279–301.

Midgley, G. F., J. N. Aranibar, K. B. Mantlana, and S. Macko (2004), Photosynthetic and gas exchange characteristics of dominant woody plants on a moisture gradient in an African savanna, *Global Change Biol.*, 10(3), 309–317, doi:10.1111/j.1365-2486.2003.00696.x.

Mielnick, P. C., and W. A. Dugas (2000), Soil CO_2 flux in a tallgrass prairie, *Soil Biol. Biochem.*, 32, 221–228.

Moncrieff, J. B., B. Monteny, A. Verhoef, T. Friborg, J. Elbers, P. Kabat, H. deBruin, H. Soegaard, P. G. Jarvis, and J. D. Taupin (1997), Spatial and temporal variations in net carbon flux during HAPEX-Sahel, *J. Hydrol.*, 189, 563–588.

National Climate Data Center (2003), Global Historical and Climatological Network, and Global Summary of the Day, Natl. Oceanic and Atmos. Admin., Boulder, Colo.

Norman, J. M. (1993), Scaling processes between leaf and canopy levels, in *Scaling Physiological Processes: Leaf to Globe*, edited by J. R. Ehleringer and C. B. Field, pp. 41–76, Academic, San Diego, Calif.

Norman, J. M., and G. S. Campbell (1989), Canopy structure, in *Plant Physiological Ecology: Field Methods and Instrumentation*, edited by R. W. Pearcy et al., pp. 301–326, Chapman and Hall, New York.

Parlange, J. Y., M. Vauclin, R. Haverkamp, and I. Lisle (1985), The relation between desorptivity and soil-water diffusivity, *Soil Sci.*, 139, 458–461.

Parlange, M. B., G. G. Katul, R. H. Cuenca, M. L. Kavvas, D. R. Nielsen, and M. Mata (1992), Physical basis for a time series model of soil water content, *Water Resour. Res.*, 28(9), 2437–2446.

Paruelo, J. M., and O. E. Sala (1995), Water losses in the Patagonian steppe—A modeling approach, *Ecology*, 76, 510–520.

Priestley, C. H. B., and R. J. Taylor (1972), On the assessment of surface heat flux and evaporation using large-scale parameters, *Mon. Weather Rev.*, 100, 81–92.

Prior, L. D., D. Eamus, and G. A. Duff (1997), Seasonal trends in carbon assimilation, stomatal conductance, pre-dawn leaf water potential and growth in Terminalia ferdinandiana, a deciduous tree of northern Australian savannas, *Aust. J. Bot.*, 45, 53–69.

Rodriguez-Iturbe, I., P. D'Odorico, A. Porporato, and L. Ridolfi (1999a), On the spatial and temporal links between vegetation, climate, and soil moisture, *Water Resour. Res.*, 35(12), 3709–3722.

Rodriguez-Iturbe, I., P. D'Odorico, A. Porporato, and L. Ridolfi (1999b), Tree-grass coexistence in savannas: The role of spatial dynamics and climate fluctuations, *Geophys. Res. Lett.*, 26(2), 247–250.

Rodriguez-Iturbe, I., A. Porporato, F. Laio, and L. Ridolfi (2001), Plants in water-controlled ecosystems: Active role in hydrologic processes and response to water stress: I. Scope and general outline, *Adv. Water Resour.*, 24, 695–705.

Rutherford, M. C. (1980), Annual plant-production precipitation relations in arid and semi-arid regions, *S. Afr. J. Sci.*, 76, 53–56.

Scanlon, T. M., and J. D. Albertson (2003a), Canopy-scale measurements of CO_2 and water vapor exchange along a precipitation gradient in southern Africa, *Global Change Biol.*, 10(3), 329–341, doi:10.1046/j.1529-8817.2003.00700.x.

Scanlon, T. M., and J. D. Albertson (2003b), Inferred controls on tree/grass composition in a savanna ecosystem: Combining 16 year normalized difference vegetation index data with a dynamic soil moisture model, *Water Resour. Res.*, 39(8), 1224, doi:10.1029/2002WR001881.

Scholes, R. J., and D. A. B. Parsons (Eds.) (1997), The Kalahari Transect: Research on global change and sustainabile development in southern

Africa, *IGBP Rep. Ser., 42*, 63 pp., Int. Geosphere-Biosphere Program, Stockholm.

Scholes, R. J., and B. H. Walker (1993), *An African Savanna: Synthesis of the Nylsvley Study*, Cambridge Univ. Press, New York.

Schulze, D. (1993), Soil water deficits and atmospheric humidity as environmental signals, in *Water Deficits: Plant Response From Cell to Community*, edited by J. A. C. Smith and H. Griffiths, pp. 129–145, BIOS Sci., Oxford, UK.

Shouse, P., W. A. Jury, L. H. Stolzy, and S. Dasberg (1982), Field measurement and modeling of cowpea water-use and yield under stressed and well-watered growth conditions, *Hilgardia*, *50*, 1–25.

Smit, G. N., and N. F. G. Rethman (2000), The influence of tree thinning on the soil water in a semi-arid savanna of southern Africa, *J. Arid Environ.*, *44*, 41–59.

Smith, T. M., H. H. Shugart, and F. J. Woodward (1997), *Plant Functional Types: Their Relevance to Ecosystem Properties and Global Change*, 369 pp., Cambridge Univ. Press, New York.

Spittlehouse, D. L., and T. A. Black (1981), A growing season water balance model applied to two Douglas fir stands, *Water Resour. Res.*, *17*(6), 1651–1656.

Tunstall, B. R., and D. J. Connor (1981), A hydrological study of a subtropical semi-arid forest of Acacia-Harpophylla F Muell Ex Benth (Brigalow), *Aust. J. Bot.*, *29*, 311–320.

van Langevelde, F., et al. (2003), Effects of fire and herbivory on the stability of savanna ecosystems, *Ecology*, *84*, 337–350.

Verhoef, A., and S. J. Allen (2000), A SVAT scheme describing energy and CO_2 fluxes for multicomponent vegetation: Calibration and test for a Sahelian savannah, *Ecol. Modell.*, *127*, 245–267.

Verhoef, A., S. J. Allen, H. A. R. DeBruin, C. M. J. Jacobs, and B. G. Heusinkveld (1996), Fluxes of carbon dioxide and water vapour from a Sahelian savanna, *Agric. For. Meteorol.*, *80*, 231–248.

Walker, B. H., D. Ludwig, C. S. Holling, and R. M. Peterman (1981), Stability of semi-arid savanna grazing systems, *J. Ecol.*, *69*, 473–498.

Webb, E., G. Pearman, and R. Leuning (1980), Correction of flux measurements for density effects due to heat and water vapour transfer, *Q. J. R. Meteorol. Soc.*, *106*, 85–100.

Wildung, R. E., T. R. Garland, and R. L. Buschborn (1975), The interdependent effects of soil temperature and water content on soil respiration rate and plant root decomposition in arid grassland soils, *Soil Biol. Biochem.*, *7*, 373–378.

————————————

J. D. Albertson, Department of Civil and Environmental Engineering, Duke University, 217 Hudson Hall, Box 90287, Durham, NC 27708, USA. (john.albertson@duke.edu)

C. A. Williams, Nicholas School of the Environment and Earth Sciences, Duke University, Durham, NC 27708-0287, USA. (christopher.a.williams@duke.edu)